Advances in Water Resources 33 (2010) 1575–1587

Contents lists available at ScienceDirect

Advances in Water Resources

journal homepage: www.elsevier.com/locate/advwatres

Hydraulics of a partially penetrating well with skin zone in a confined aquifer

Gautam Barua [a,*], S.N. Bora [b]

[a] Department of Civil Engineering, Indian Institute of Technology Guwahati, Guwahati 781 039, Assam, India
[b] Department of Mathematics, Indian Institute of Technology Guwahati, Guwahati 781 039, Assam, India

ARTICLE INFO

Article history:
Received 18 March 2010
Received in revised form 15 September 2010
Accepted 17 September 2010
Available online 25 September 2010

Keywords:
Hydraulic conductivity
Skin thickness
Steady/quasi-steady state
Horizontal and vertical extent of aquifer
Pumping test

ABSTRACT

A steady/quasi-steady model is developed for predicting flow into a partially penetrating well with skin zone in a confined aquifer overlying an impervious layer. The model takes into account flow through the bottom of the wellbore, finite skin thickness and finite horizontal and vertical extent of the aquifer. Moreover, the solution can be easily extended to include the mixed-type boundary condition at the well face, where a Dirichlet in the form of a specified hydraulic head and a Neumann in the form of zero flux coexist at the same time at different portions of the well face. The validity of the proposed solution is tested by comparing a few results obtained from the developed model with corresponding results obtained by analytical and numerical means. The study shows that, among other factors remaining constant, both the horizontal and vertical extent of an artesian aquifer, thickness of the skin zone, bottom flow and conductivity contrast of the skin and formation zones, play an important part in deciding flow to a well dug in the aquifer, and hence these factors must be considered while analyzing the problem. The model proposed here can be used to estimate skin thickness as well as hydraulic conductivities of the skin and formation zones of a well with skin zone in an artesian aquifer underlain by an impervious layer by utilizing pumping test data falling in the steady or quasi-steady state of a typical pumping test. As the proposed solution is of a general nature in the sense that it can handle, apart from partial penetration and bottom flow, the finite size skin zone and finite horizontal and vertical extent of an artesian aquifer together with the mixed-type boundary condition at the well face, it is hoped that the predictions coming out of the model will be more realistic than those obtained using solutions developed with more stringent assumptions.

1. Introduction

An accurate estimation of various hydraulic parameters associated with an aquifer in its natural state is of fundamental importance in obtaining rational solutions to various problems associated with groundwater seepage through the aquifer, including contaminant transport. Estimates of directional conductivities of an aquifer are used as inputs in numerous analytical and numerical models related to groundwater movement through the aquifer. A model is as accurate as the accuracy of its inputs, no matter whatever might be the level of sophistication of the model. Thus, a correct estimate of the various parameters involved in a model is of considerable importance, as error in the inputs may be reflected, sometimes in many folds, in the outputs from the model. One of the most commonly adopted methods of aquifer parameter estimation is the pumping test. The method essentially consists of imposing a stress in an aquifer by pumping it and then monitoring the responses of the water level with time in the pumping well and/or in piezometer(s) around the well. These responses are then fed into some parameter estimation model as inputs and the parameters sought after are then estimated as outputs from these models.

The traditional approach of solving the transient groundwater flow problem into a well fully or partially penetrating an aquifer is to solve a diffusion equation [35] subjected to a Neumann along the well face ([16,18,24–26] – to name a few). Actually the boundary value problem associated with a well partially penetrating an aquifer is of a mixed-type with a Dirichlet ([5,6,8,15,19,35,38] and others) specified at the screened and a Neumann at the unscreened portions of the well. Dagan [15] provided a steady state semi-analytic solution to the mixed-boundary partially penetrating well hydraulics problem for a phreatic aquifer by adopting the Green's function method; this solution, however, has the limitation [38,40] that the active length of the well must be much larger (50 times or more) than the radius of the well screen for the solution to work correctly. Widdowson et al. [38] and Ruud and Kabala [35] presented numerical solutions to the non-uniform radial flux problem for an artesian aquifer and Hemker [19] provided a hybrid analytical–numerical solution to the mixed-boundary problem for a vertically heterogeneous artesian aquifer. Chang

* Corresponding author. Tel.: +91 361 258 2413; fax: +91 361 258 2440.
E-mail addresses: g_barua@iitg.ernet.in (G. Barua), swaroop@iitg.ernet.in (S.N. Bora).

0309-1708/$ - see front matter © 2010 Elsevier Ltd. All rights reserved.
doi:10.1016/j.advwatres.2010.09.008

Nomenclature

$A_m, B_n, C_p, D_q, B_0, C_0, D_0$	constants with $m = 1,2,3,\ldots$, $n = 1,2,3,\ldots$, $p = 1,2,3,\ldots$, $q = 1,2,3,\ldots$
a	radius of the well of Fig. 1, L
b	horizontal extent of the aquifer as measured from the centre of the well of Fig. 1, L
h	depth to the impervious layer as measured from the top of the confining stratum of Fig. 1, L
H_3	depth of penetration of the well as measured from the top of the confining stratum of Fig. 1, L
$I_0(\cdot), I_1(\cdot)$	zero and first order modified Bessel functions of first kind, respectively
K	hydraulic conductivity of homogeneous and isotropic aquifer, $L\,T^{-1}$
K_f	isotropic hydraulic conductivity of zone R-3 of Fig. 1, $L\,T^{-1}$
K_s	isotropic hydraulic conductivity of zones R-2 and R-3 of Fig. 1, $L\,T^{-1}$
K_{ri}	horizontal hydraulic conductivity of the ith region (R-i) of Fig. 1, $i = 1,2,3$, $L\,T^{-1}$
K_r	horizontal hydraulic conductivity of homogeneous anisotropic aquifer, $L\,T^{-1}$
K_{zi}	vertical hydraulic conductivity of the ith region (R-i) of Fig. 1, $i = 1,2,3$, $L\,T^{-1}$
K_z	vertical hydraulic conductivity of homogeneous anisotropic aquifer, $L\,T^{-1}$
$(K'_0)^2$	K_r/K_z
$K^{(i)}$	K_{ri}/K_{zi}, anisotropy ratio for the ith region of Fig. 1, $i = 1,2,3$
K_{2-3}	isotropic hydraulic conductivity of the regions R-2 and R-3 of Fig. 1, $L\,T^{-1}$
$K_0(\cdot), K_1(\cdot)$	zero and first order modified Bessel functions of second kind, respectively
M, N, P, Q^I	number of terms to be summed in the series solution, $1,2,3,\ldots$
N_{pz}	number of piezometer readings considered for the inverse modeling
Q	total discharge of the well of Fig. 1, $L^3\,T^{-1}$
Q_b	discharge through the bottom of the well of Fig. 1, $L^3\,T^{-1}$
Q_s	discharge through the sides of the well of Fig. 1, $L^3\,T^{-1}$
Q_C	total discharge of the well due to Cassiani et al.'s theory [6] for specific flow situations of Fig. 1, $L^3\,T^{-1}$
Q_T	total discharge of the well of Fig. 1 due to Thiem's equation, $L^3\,T^{-1}$
r	radial coordinate as measured from the centre of the well, L
s	distance of the outer edge of the skin zone as measured from the centre of the well of Fig. 1, L
h_a	hydraulic head of the confined aquifer with respect to the origin of Fig. 1 prior to pumping, L
h_0	steady/quasi-steady hydraulic head of the pumping well with respect to the origin of Fig. 1, L
z	vertical coordinate as measured from the top of the confining stratum of Fig. 1, L
θ	K_f/K_s, hydraulic conductivity ratio between the skin and formation zones
ϕ_i	hydraulic head distribution for the ith region (R-i) of Fig. 1, $i = 1,2,3$, L
ψ_i	stream function for the ith region (R-i) of Fig. 1, $i = 1,2,3$, $L^2\,T^{-1}$
ψ_i^n	normalized stream function for the ith region (R-i) of Fig. 1, $i = 1,2,3$

Subscripts

1, 2	related to zones R-2 and R-3 of Fig. 1
3	related to formation zone of Fig. 1

and Chen [8] provided an analytical solution to the transient mixed-boundary problem at the well face for a flowing partially penetrating well in an artesian aquifer of infinite horizontal extent by adopting a well screen discretization method, similar to the one adopted by others [15,17,23,37] to solve different boundary value problems. Chang and Yeh [9] obtained a semi-analytical solution to the constant-head partially penetrating well hydraulics problem for a confined aquifer of infinite radial extend and finite vertical extent by making use of the dual series and perturbation methods. Their solution has the ability to tackle the mixed-type boundary condition at the well face without resorting to discretization of the well screen. However, this solution is valid only for the situation when the well screen starts from the top of the confining stratum. To address this limitation, Chang and Yeh [10] provided a new triple series analytical solution to the constant-head partially penetrating well hydraulics problem where they could successfully include any arbitrary location of the well screen at the well face in their mathematical model.

Pumping tests conducted in a low storativity aquifer have been observed to be influenced by a zone of permeability reduction (positive skin) or enhancement (negative skin) in the neighborhood of the pumping well [29,30,39,41–44] and hence this zone must be accounted for in the theoretical analysis of the problem. A skin region is generally formed during drilling of a well as a result of drilling mud or rock flour invasion and as such this zone has a lower conductivity (positive skin) than the formation zone. However, in some circumstances, a zone of higher conductivity (negative skin) in the immediate vicinity of a well as compared to regions farther away from the well may also develop due to extensive spalling and fracturing of the wellbore during drilling and/or due to extensive well development [29,30,39,41–44]. The skin hydraulics problem for an aquifer of infinite horizontal dimension was solved analytically by several investigators [5,6,11,13,14,20,29,31–33,39,41–44] utilizing different assumptions. Whereas Novakowski [29], Yang and Yeh [39], Yeh et al. [43], Cimen [14] and Yeh and Yang [44] provided analytical solutions to the problem by neglecting vertical flow, Novakowski [31] provided a solution by assigning a specified head on the well face but a zero head and not a zero flux in the non-active portion of the well, and Hyder et al. [20], Yang and Yeh [41], Chiu et al. [13], Yeh et al. [42] and Chang et al. [11] presented solutions by assuming a uniform radial flux at the well screen. Cassiani et al. [6], using the dual integral method of Cassiani and Kabala [5], presented a semi-analytical solution to the transient skin hydraulics problem for a confined aquifer with a mixed-boundary at the well face by assuming the skin to be infinitesimal small and the aquifer to be infinite in both horizontal and vertical directions. Further, they also assumed the bottom of the wellbore to not collect any water during their analysis. Chang and Chen [7] later provided a solution to the same problem for an aquifer with finite vertical extent using appropriate integral transforms but the other assumptions remained in their solution as well. Perina and Lee [33] provided a general solution to the problem which can incorporate skin thickness, partial penetration, leaky boundary flux for both confined and unconfined situations and the mixed-boundary at the well face. However, they also assumed the outer zone to extend to infinity and the bottom of the wellbore to not collect any flow from the aquifer in their analysis as had been assumed by Cassiani and Kabala [5] and Cassiani

et al. [6] in their analytical development. Pasandi et al. [32] solved the skin hydraulics problem for a partially penetrating well in a phreatic aquifer but here also the well screen flux was assumed to be independent of the vertical ordinate, the aquifer to be of infinite horizontal extent and the bottom of the wellbore to not collect any water from the aquifer in the analysis. In this paper, we propose to develop a general steady state analytical solution to the partially penetrating well hydraulics problem for a confined aquifer with a finite skin by incorporating bottom flow as well as finite horizontal and vertical extent of the aquifer into the solution. Further, we propose to develop our analytical model without taking resort to the assumption of a uniform flux at the well face. As a steady state solution is equally applicable for quasi-steady situations [4,22,27,28], when the hydraulic heads vary in space and time but the hydraulic gradients vary only in space, it is hoped that the proposed model will also be of use in interpreting quasi-steady pumping test results as well. This is important because a well in a confined aquifer may require a very large pumping time for steady state to be reached whereas quasi-steady states may be reached in a relatively much shorter time [22] after the initiation of pumping. The developed model is also expected to throw some light on the effect of the outer zone and bottom flow on the overall flow hydraulics of a partially penetrating well in a confined aquifer with skin zone.

2. Mathematical formulation and solution

Fig. 1 shows the geometry of the problem under consideration. A well of radius a and a wellbore skin thickness of $s - a$ penetrates a confined aquifer of uniform thickness h, where s is the distance of the skin zone from the centre of the well. The well is underlain by an impervious layer and the well penetration is taken as H_3, the distance being measured from the top of the confining stratum as shown in the figure. The hydraulic head at the well face and on a vertically concentric cylindrical surface located at a distance b from the centre of the well are taken as h_0 and h_a, respectively. The flow domain of interest is the one shown in the figure, but because of axial symmetry we consider only one half of the flow domain for analysis. For convenience, we take the z-axis to be positive vertically downward and the r axis to be positive towards the right. Further, for ease of solution, we split the flow domain into three sub-domains R-1, R-2 and R-3, respectively, as shown in the figure. The horizontal and vertical hydraulic conductivities in these regions are denoted by K_{ri} and K_{zi} ($i = 1,2,3$), respectively, and the hydraulic heads by ϕ_1, ϕ_2 and ϕ_3, respectively. In the analysis presented here, we assume the flow to be steady, the aquifer material and water to be incompressible and the principal directions of anisotropy to coincide with the horizontal and vertical directions in all the three regions R-1, R-2 and R-3 of the flow domain. Also, we assume the skin zone R-2 to extend all the way up to the impervious layer. If the blind section of casing extends all the way up to the impervious layer, then the associated no-flow condition can be introduced in an indirect way as will be made clear later in our analysis.

The solution to the boundary value problem, as shown in Fig. 1, requires evaluation of the hydraulic head functions ϕ_1, ϕ_2 and ϕ_3 for R-1, R-2 and R-3, respectively, in such a way that the following governing equations are satisfied

$$K_{ri}\frac{\partial^2\phi_i}{\partial r^2}+\frac{K_{ri}}{r}\frac{\partial\phi_i}{\partial r}+K_{zi}\frac{\partial^2\phi_i}{\partial z^2}=0,\quad i=1,2,3, \tag{1}$$

together with the boundary conditions as listed below

$$\frac{\partial\phi_1}{\partial r}=0,\quad r=0,\ H_3<z<h, \tag{I}$$
$$\phi_1=h_0,\quad z=H_3,\ 0<r<a, \tag{II}$$
$$\frac{\partial\phi_1}{\partial z}=0,\quad z=h,\ 0<r<a, \tag{III}$$
$$\frac{\partial\phi_2}{\partial z}=0,\quad z=0,\ a<r<s, \tag{IV}$$
$$\frac{\partial\phi_2}{\partial z}=0,\quad z=h,\ a<r<s, \tag{V}$$
$$\phi_2=h_0,\quad r=a,\ 0<z<H_3, \tag{VI}$$
$$\frac{\partial\phi_3}{\partial z}=0,\quad z=0,\ s<r<b, \tag{VII}$$
$$\frac{\partial\phi_3}{\partial z}=0,\quad z=h,\ s<r<b, \tag{VIII}$$
$$\phi_3=h_a,\quad r=b,\ 0<z<h. \tag{IX}$$

Further, apart from the boundary conditions stated above, continuity demands that the hydraulic head functions ϕ_1, ϕ_2 and ϕ_3 sought to be evaluated must also satisfy the following interfacial conditions at the interfaces of R-1 and R-2, and R-2 and R-3 of Fig. 1

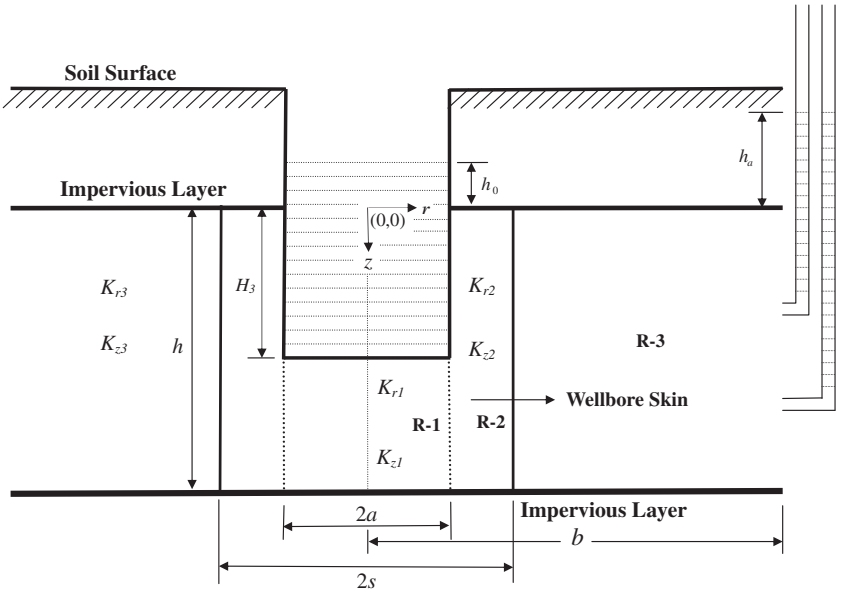

Fig. 1. Geometry of a partially penetrating well with skin zone in a confined aquifer.

$$\phi_1 = \phi_2, \quad r = a,\ H_3 < z < h, \tag{X}$$

$$K_{r1}\frac{\partial \phi_1}{\partial r} = K_{r2}\frac{\partial \phi_2}{\partial r}, \quad r = a,\ H_3 < z < h, \tag{XI}$$

$$\phi_2 = \phi_3, \quad r = s,\ 0 < z < h \tag{XII}$$

$$K_{r2}\frac{\partial \phi_2}{\partial r} = K_{r3}\frac{\partial \phi_3}{\partial r}, \quad r = s,\ 0 < z < h. \tag{XIII}$$

Taking into consideration the above boundary and interfacial conditions, the hydraulic head expressions for the regions R-1, R-2 and R-3 of Fig. 1 satisfying Eq. (1) may be expressed as (see Appendix)

$$\phi_1 = \sum_{m=1}^{M} A_m \frac{I_0\left\{\frac{-N_m r}{K^{(1)}}\right\}}{I_0\left\{\frac{-N_m a}{K^{(1)}}\right\}} \sin\{N_m(z - H_3)\} + h_0, \tag{2}$$

$$\phi_2 = \sum_{n=1}^{N} B_n \left\{\frac{K_0\left(\frac{N_n s}{K^{(2)}}\right) I_0\left(\frac{N_n r}{K^{(2)}}\right) - K_0\left(\frac{N_n r}{K^{(2)}}\right) I_0\left(\frac{N_n s}{K^{(2)}}\right)}{K_0\left(\frac{N_n s}{K^{(2)}}\right) I_0\left(\frac{N_n a}{K^{(2)}}\right) - K_0\left(\frac{N_n a}{K^{(2)}}\right) I_0\left(\frac{N_n s}{K^{(2)}}\right)}\right\} \cos(N_n z) + B_0 \frac{\log_e\left(\frac{s}{r}\right)}{\log_e\left(\frac{s}{a}\right)}$$
$$+ \sum_{q=1}^{Q'} D_q \left\{\frac{K_0\left(\frac{N_q a}{K^{(2)}}\right) I_0\left(\frac{N_q r}{K^{(2)}}\right) - K_0\left(\frac{N_q r}{K^{(2)}}\right) I_0\left(\frac{N_q a}{K^{(2)}}\right)}{K_0\left(\frac{N_q a}{K^{(2)}}\right) I_0\left(\frac{N_q s}{K^{(2)}}\right) - K_0\left(\frac{N_q s}{K^{(2)}}\right) I_0\left(\frac{N_q a}{K^{(2)}}\right)}\right\} \cos(N_q z + D_0 \frac{\log_e\left(\frac{a}{r}\right)}{\log_e\left(\frac{a}{s}\right)} \tag{3}$$

and

$$\phi_3 = \sum_{p=1}^{P} C_p \left\{\frac{K_0\left(\frac{N_p b}{K^{(3)}}\right) I_0\left(\frac{N_p r}{K^{(3)}}\right) - K_0\left(\frac{N_p r}{K^{(3)}}\right) I_0\left(\frac{N_p b}{K^{(3)}}\right)}{K_0\left(\frac{N_p b}{K^{(3)}}\right) I_0\left(\frac{N_p s}{K^{(3)}}\right) - K_0\left(\frac{N_p s}{K^{(3)}}\right) I_0\left(\frac{N_p b}{K^{(3)}}\right)}\right\} \cos(N_p z)$$
$$- C_0 \frac{\log_e\left(\frac{b}{r}\right)}{\log_e\left(\frac{b}{s}\right)} + h_a, \tag{4}$$

where

$$N_m = \left\{\frac{(1-2m)\pi}{2(h - H_3)}\right\}, \tag{5}$$

$$N_n = \left(\frac{n\pi}{h}\right), \tag{6}$$

$$N_q = \left(\frac{q\pi}{h}\right), \tag{7}$$

$$N_p = \left(\frac{p\pi}{h}\right) \tag{8}$$

and the other symbols of the hydraulic head expressions have already been defined in the Appendix.

The boundary value problem considered here may be visualized as an extension of the steady state partially penetrating well hydraulics problem considered by Kirkham [21] and Barua and Hofffmann [1] for the no-skin situation (R-2 = 0) where only regions R-1 and R-3 were considered for the analytical development. Here, an effort is made to solve the same problem by infusing region R-2 in the problem domain in between R-1 and R-3.

We will now evaluate the constants A_m, B_n, C_p, D_q, B_0, C_0 and D_0 of Eqs. (2)–(4) using conditions X, XI, VI, XII and XIII as stated above. Applying interfacial condition (XII) to Eqs. (3) and (4), respectively, we obtain, at $r = s$

$$D_0 + \sum_{q=1}^{Q'} D_q \cos(N_q z) = \sum_{p=1}^{P} C_p \cos(N_p z) - C_0 + h_a, \quad 0 < z < h. \tag{9}$$

By letting $Q' \to \infty$ [in view of Eq. (A14)], the constants D_0 and D_q may then be evaluated by running a Fourier cosine series in the interval $0 < z < h$ to yield

$$D_0 = \frac{1}{h}\left\{\int_0^h (-C_0 + h_a)dz + \int_0^h \sum_{p=1}^{P} C_p \cos(N_p z)dz\right\} \tag{10}$$

and

$$D_q = \frac{2}{h}\left\{\int_0^h \sum_{p=1}^{P} C_p \cos(N_p z)\cos(N_q z)dz + \int_0^h (-C_0 + h_a)\cos(N_q z)dz\right\}. \tag{11}$$

Eqs. (10) and (11), upon simplification, give

$$D_0 = (-C_0 + h_a) \tag{12}$$

and

$$D_q = C_q. \tag{13}$$

Now, applying condition (XIII) to Eqs. (3) and (4), respectively, we obtain

$$\sum_{p=1}^{P} C_p \left(\frac{K_{r3}}{K^{(3)}}\right) Z_{3(p)} \cos(N_p z) + \left(\frac{C_0}{s}\right)\left\{\frac{K_{r3}}{\log_e\left(\frac{b}{s}\right)}\right\}$$
$$= \sum_{n=1}^{N} B_n \left(\frac{K_{r2}}{K^{(2)}}\right) Z_{2(n)} \cos(N_n z) - \left(\frac{B_0}{s}\right)\left\{\frac{K_{r2}}{\log_e\left(\frac{s}{a}\right)}\right\}$$
$$+ \sum_{q=1}^{Q'} D_q \left(\frac{K_{r2}}{K^{(2)}}\right) Z_{1(q)} \cos(N_q z) - \left(\frac{D_0}{s}\right)\left\{\frac{K_{r2}}{\log_e\left(\frac{a}{s}\right)}\right\}, \quad 0 < z < h, \tag{14}$$

where

$$Z_{1(q)} = (N_q)\left\{\frac{K_0\left(\frac{N_q a}{K^{(2)}}\right) I_1\left(\frac{N_q s}{K^{(2)}}\right) + K_1\left(\frac{N_q s}{K^{(2)}}\right) I_0\left(\frac{N_q a}{K^{(2)}}\right)}{K_0\left(\frac{N_q a}{K^{(2)}}\right) I_0\left(\frac{N_q s}{K^{(2)}}\right) - K_0\left(\frac{N_q s}{K^{(2)}}\right) I_0\left(\frac{N_q a}{K^{(2)}}\right)}\right\}, \tag{15}$$

$$Z_{2(n)} = (N_n)\left\{\frac{K_0\left(\frac{N_n s}{K^{(2)}}\right) I_1\left(\frac{N_n s}{K^{(2)}}\right) + K_1\left(\frac{N_n s}{K^{(2)}}\right) I_0\left(\frac{N_n s}{K^{(2)}}\right)}{K_0\left(\frac{N_n s}{K^{(2)}}\right) I_0\left(\frac{N_n a}{K^{(2)}}\right) - K_0\left(\frac{N_n a}{K^{(2)}}\right) I_0\left(\frac{N_n s}{K^{(2)}}\right)}\right\}, \tag{16}$$

$$Z_{3(p)} = (N_p)\left\{\frac{K_0\left(\frac{N_p b}{K^{(3)}}\right) I_1\left(\frac{N_p s}{K^{(3)}}\right) + K_1\left(\frac{N_p s}{K^{(3)}}\right) I_0\left(\frac{N_p b}{K^{(3)}}\right)}{K_0\left(\frac{N_p b}{K^{(3)}}\right) I_0\left(\frac{N_p s}{K^{(3)}}\right) - K_0\left(\frac{N_p s}{K^{(3)}}\right) I_0\left(\frac{N_p b}{K^{(3)}}\right)}\right\} \tag{17}$$

and $I_1(\cdot)$ and $K_1(\cdot)$ are first order modified Bessel functions of first and second kinds, respectively.

Now, letting $P \to \infty$ and once again running a Fourier cosine series in the interval $0 < z < h$, the constants C_0 and C_p can then be determined as

$$\left(\frac{C_0}{s}\right)\left\{\frac{K_{r3}}{\log_e\left(\frac{b}{s}\right)}\right\}$$
$$= \frac{1}{h}\int_0^h \left\{\sum_{n=1}^{N} B_n \left(\frac{K_{r2}}{K^{(2)}}\right) Z_{2(n)} \cos(N_n z) - \left(\frac{B_0}{s}\right)\left[\frac{K_{r2}}{\log_e\left(\frac{s}{a}\right)}\right]\right\} dz$$
$$+ \frac{1}{h}\int_0^h \left\{\sum_{q=1}^{Q'} D_q \left(\frac{K_{r2}}{K^{(2)}}\right) Z_{1(q)} \cos(N_q z) - \left(\frac{D_0}{s}\right)\left[\frac{K_{r2}}{\log_e\left(\frac{a}{s}\right)}\right]\right\} dz, \tag{18}$$

$$C_p \left(\frac{K_{r3}}{K^{(3)}}\right) Z_{3(p)}$$
$$= \frac{2}{h}\int_0^h \left\{\sum_{n=1}^{N} B_n \left(\frac{K_{r2}}{K^{(2)}}\right) Z_{2(n)} \cos(N_n z) - \left(\frac{B_0}{s}\right)\left[\frac{K_{r2}}{\log_e\left(\frac{s}{a}\right)}\right]\right\} \cos(N_p z)dz$$
$$+ \frac{2}{h}\int_0^h \left\{\sum_{q=1}^{Q'} D_q \left(\frac{K_{r2}}{K^{(2)}}\right) Z_{1(q)} \cos(N_q z) - \left(\frac{D_0}{s}\right)\left[\frac{K_{r2}}{\log_e\left(\frac{a}{s}\right)}\right]\right\} \cos(N_p z)dz. \tag{19}$$

Simplifying Eqs. (18) and (19) by utilizing the results of Eqs. (12) and (13), we get

$$C_0 = -\left\{\frac{\frac{h_a K_{r2}}{\log_e\left(\frac{a}{s}\right)} + \frac{B_0 K_{r2}}{\log_e\left(\frac{s}{a}\right)}}{\frac{K_{r3}}{\log_e\left(\frac{b}{s}\right)} - \frac{K_{r2}}{\log_e\left(\frac{a}{s}\right)}}\right\} \tag{20}$$

and

$$C_n = \left\{\frac{B_n\left(\frac{K_{r2}Z_{2(n)}}{K^{(2)}}\right)}{\left(\frac{K_{r3}Z_{3(n)}}{K^{(3)}}\right) - \left(\frac{K_{r2}Z_{1(n)}}{K^{(2)}}\right)}\right\}, \tag{21}$$

where it is to be noted that the integrals of Eq. (19) survive only when $N_p = N_q = N_n$ (i.e., when $p = q = n$).

Now, applying conditions (X) and (VI) at $r = a$ to ϕ_1 and ϕ_2, respectively, we get

$$B_0 + \sum_{n=1}^{N} B_n \cos(N_n z) = h_0, \quad 0 < z < H_3 \tag{22}$$

and

$$B_0 + \sum_{n=1}^{N} B_n \cos(N_n z) = \sum_{m=1}^{M} A_m \sin\{N_m(z - H_3)\} + h_0, \quad H_3 \leqslant z < h. \tag{23}$$

The constants B_0 and B_n can be worked out, like before, by applying a Fourier series in the interval $0 < z < h$ – the integral expressions turn out to be

$$B_0 = \frac{1}{h}\left\{\int_0^{H_3}(h_0)dz + \int_{H_3}^{h}\left[\sum_{m=1}^{M} A_m \sin[N_m(z - H_3)] + h_0\right]dz\right\} \tag{24}$$

and

$$B_n = \frac{2}{h}\left\{\int_0^{H_3} h_0 \cos(N_n z)dz + \int_{H_3}^{h} h_0 \cos(N_n z)dz + \int_{H_3}^{h}\sum_{m=1}^{M} A_m \sin[N_m(z - H_3)]\cos(N_n z)dz\right\}. \tag{25}$$

Carrying out the integration in Eq. (24), we get

$$B_0 = h_0 + \frac{1}{h}\sum_{m=1}^{M}\left(\frac{A_m}{N_m}\right). \tag{26}$$

Eq. (25), upon simplification, gives, for $N_m^2 \neq N_n^2$

$$B_n = \frac{2}{h}\left\{\sum_{m=1}^{M} A_m\left[\frac{-\cos[(N_m - N_n)h - (N_m H_3)]}{2(N_m - N_n)} - \frac{\cos[(N_m + N_n)h - (N_m H_3)]}{2(N_m + N_n)} + \frac{N_m}{\left(N_m^2 - N_n^2\right)}\cos(N_n H_3)\right]\right\} \tag{27}$$

and, for $N_n = |N_m|$, we have

$$B_n = \frac{2}{h}\left\{\sum_{m=1}^{M} A_m\left[\frac{\cos(N_m H_3)}{4N_m}[1 - \cos(2N_m h)] - \left(\frac{h - H_3}{2}\right)\sin(N_m H_3)\right]\right\}. \tag{28}$$

For brevity, we express Eq. (27), for $N_m^2 \neq N_n^2$, as

$$B_n = \frac{2}{h}\sum_{m=1}^{M} A_m P_{mn} \tag{29}$$

and Eq. (28), for $N_n = |N_m|$, as

$$B_n = \frac{2}{h}\sum_{m=1}^{M} A_m P_{m=n}, \tag{30}$$

where

$$P_{mn} = \left\{\frac{-\cos[(N_m - N_n)h - (N_m H_3)]}{2(N_m - N_n)} - \frac{\cos[(N_m + N_n)h - (N_m H_3)]}{2(N_m + N_n)} + \frac{N_m}{\left(N_m^2 - N_n^2\right)}\cos(N_n H_3)\right\} \tag{31}$$

and

$$P_{m=n} = \left\{\frac{\cos(N_m H_3)}{4N_m}[1 - \cos(2N_m h)] - \left(\frac{h - H_3}{2}\right)\sin(N_m H_3)\right\}. \tag{32}$$

We now use condition (XI) to generate the remaining set of relations among the constants A_m, B_n – this condition, when applied to Eqs. (2) and (3), respectively, yields

$$\sum_{m=1}^{M} A_m\left(\frac{K_{r1}}{K^{(1)}}\right)Z_{4(m)}\sin\{N_m(z - H_3)\} = \sum_{n=1}^{N} B_n\left(\frac{K_{r2}}{K^{(2)}}\right)Z_{6(n)}\cos(N_n z) - \left(\frac{B_0}{a}\right)\left\{\frac{K_{r2}}{\log_e\left(\frac{s}{a}\right)}\right\} + \sum_{q=1}^{Q'} D_q\left(\frac{K_{r2}}{K^{(2)}}\right)Z_{5(q)}\cos(N_q z) - \left(\frac{D_0}{a}\right)\left\{\frac{K_{r2}}{\log_e\left(\frac{a}{s}\right)}\right\}, \tag{33}$$

where

$$Z_{4(m)} = (-N_m)\left\{\frac{I_1\left(\frac{-N_m a}{K^{(1)}}\right)}{I_0\left(\frac{-N_m a}{K^{(1)}}\right)}\right\}, \tag{34}$$

$$Z_{5(q)} = (N_q)\left\{\frac{K_0\left(\frac{N_q a}{K^{(2)}}\right)I_1\left(\frac{N_q a}{K^{(2)}}\right) + K_1\left(\frac{N_q a}{K^{(2)}}\right)I_0\left(\frac{N_q a}{K^{(2)}}\right)}{K_0\left(\frac{N_q a}{K^{(2)}}\right)I_0\left(\frac{N_q s}{K^{(2)}}\right) - K_0\left(\frac{N_q s}{K^{(2)}}\right)I_0\left(\frac{N_q a}{K^{(2)}}\right)}\right\} \tag{35}$$

and

$$Z_{6(n)} = (N_n)\left\{\frac{K_0\left(\frac{N_n s}{K^{(2)}}\right)I_1\left(\frac{N_n a}{K^{(2)}}\right) + K_1\left(\frac{N_n a}{K^{(2)}}\right)I_0\left(\frac{N_n s}{K^{(2)}}\right)}{K_0\left(\frac{N_n s}{K^{(2)}}\right)I_0\left(\frac{N_n a}{K^{(2)}}\right) - K_0\left(\frac{N_n a}{K^{(2)}}\right)I_0\left(\frac{N_n s}{K^{(2)}}\right)}\right\}. \tag{36}$$

Now letting $M \to \infty$, we can carry out a Fourier expansion [1] along the boundary $H_3 < z < h$ and the constants A_m can then be evaluated as

$$\begin{aligned} A_m\left(\frac{K_{r1}}{K^{(1)}}\right)Z_{4(m)} = {} & \left\{\frac{2}{(h - H_3)}\right\}\int_{H_3}^{h}\sum_{n=1}^{N} B_n\left(\frac{K_{r2}}{K^{(2)}}\right)Z_{6(n)}\cos(N_n z) \times \sin\{N_m(z - H_3)\}dz + \left\{\frac{2}{(h - H_3)}\right\} \\ & \times \int_{H_3}^{h}\sum_{q=1}^{Q'} D_q\left\{\frac{K_{r2}}{K^{(2)}}\right\}Z_{5(q)}\cos(N_q z)\sin\{N_m(z - H_3)\}dz \\ & - \left\{\frac{2}{(h - H_3)}\right\}\left(\frac{B_0}{a}\right)\left\{\frac{K_{r2}}{\log_e\left(\frac{s}{a}\right)}\right\}\int_{H_3}^{h}\sin\{N_m(z - H_3)\}dz \\ & - \left\{\frac{2}{(h - H_3)}\right\}\left(\frac{D_0}{a}\right)\left\{\frac{K_{r2}}{\log_e\left(\frac{a}{s}\right)}\right\}\int_{H_3}^{h}\sin\{N_m(z - H_3)\}dz. \end{aligned} \tag{37}$$

Simplifying Eq. (37) by using Eqs. (12), (13), (20), (21) and (26), we have, for $N_m^2 \neq N_n^2$

$$A_m = \left\{\frac{2K^{(1)}}{K_{r1}Z_{4(m)}(h-H_3)}\right\}\left\{\sum_{n=1}^{N} B_n \frac{\left(\frac{K_{r2}Z_{2(n)}}{K^{(2)}}\right)}{\left[\left(\frac{K_{r3}Z_{3(n)}}{K^{(3)}}\right)-\left(\frac{K_{r2}Z_{1(n)}}{K^{(2)}}\right)\right]}\left(\frac{Z_{5(n)}K_{r2}P_{mn}}{K^{(2)}}\right)\right\} + \left\{\frac{2K^{(1)}}{K_{r1}Z_{4(m)}(h-H_3)}\right\}\left\{\sum_{n=1}^{N} B_n\left(\frac{Z_{6(n)}K_{r2}P_{mn}}{K^{(2)}}\right)\right\} - W_1W_{3(m)} - (W_{4(m)}+W_2W_{3(m)})h_0 - \left\{\frac{(W_{4(m)}+W_2W_{3(m)})}{h}\right\}\sum_{u=1}^{N}\left(\frac{A_u}{N_u}\right), \tag{38}$$

where

$$W_1 = \left\{\frac{\frac{h_aK_{r2}}{\log_e\left(\frac{a}{s}\right)}}{\frac{K_{r3}}{\log_e\left(\frac{b}{s}\right)}-\frac{K_{r2}}{\log_e\left(\frac{a}{s}\right)}}\right\}+h_a, \tag{39}$$

$$W_2 = \left\{\frac{\frac{K_{r2}}{\log_e\left(\frac{s}{a}\right)}}{\frac{K_{r3}}{\log_e\left(\frac{b}{s}\right)}-\frac{K_{r2}}{\log_e\left(\frac{a}{s}\right)}}\right\}, \tag{40}$$

$$W_{3(m)} = \left\{\frac{2K_{r2}K^{(1)}}{Z_{4(m)}N_mK_{r1}a\log_e\left(\frac{a}{s}\right)(h-H_3)}\right\}, \tag{41}$$

$$W_{4(m)} = \left\{\frac{2K_{r2}K^{(1)}}{Z_{4(m)}N_mK_{r1}a\log_e\left(\frac{s}{a}\right)(h-H_3)}\right\}, \tag{42}$$

$$N_u = \left\{\frac{(1-2u)\pi}{2(h-H_3)}\right\} \tag{43}$$

and $N = M = P = Q^I$ is taken so the number of equations remains equal to the number of unknowns.

For $N_n = |N_m|$, the equation linking A_m and B_n is the same as Eq. (38), except that P_{mn} in it should now be replaced by $P_{m=n}$ of Eq. (32). It should be noted that even though we have presented here equations for the situation $N_n = |N_m|$ for completeness, in actual applications such a situation can be easily avoided by a judicious adjustment of the flow parameters h and H_3. Linear equations originating from Eqs. (27) and (38) can now be solved to evaluate A_m and B_n following a Gauss elimination procedure or by some other suitable means [36]; once A_m and B_n are being determined, C_n [and hence D_n since $D_q = C_q$; Eq. (13)], B_0, C_0 and D_0 can next be worked out utilizing Eqs. (21), (26), (20) and (12), respectively. Thus, our boundary value problem stands solved for the hydraulic head function. Now, to get the Stoke's stream functions, ψ_i, from the derived hydraulic head function, ϕ_i, we use the following relations for axis-symmetric flow for a homogeneous and anisotropic soil medium [3]:

$$K_r\frac{\partial\phi}{\partial r} = \frac{1}{r}\frac{\partial\psi}{\partial z} \tag{44}$$

and

$$K_z\frac{\partial\phi}{\partial z} = -\frac{1}{r}\frac{\partial\psi}{\partial r}. \tag{45}$$

Applying Eqs. (44) and (45) to Eqs. (2)–(4), respectively, we get

$$\psi_1 = \sum_{m=1}^{M} A_m\left(\frac{rK_{r1}}{K^{(1)}}\right)\frac{I_1\left(\frac{-N_mr}{K^{(1)}}\right)}{I_0\left(\frac{-N_ma}{K^{(1)}}\right)}\cos\{N_m(z-H_3)\}, \tag{46}$$

$$\psi_2 = \sum_{n=1}^{N} B_n\left(\frac{rK_{r2}}{K^{(2)}}\right)\left\{\frac{K_0\left(\frac{N_ns}{K^{(2)}}\right)I_1\left(\frac{N_nr}{K^{(2)}}\right)+K_1\left(\frac{N_nr}{K^{(2)}}\right)I_0\left(\frac{N_ns}{K^{(2)}}\right)}{K_0\left(\frac{N_ns}{K^{(2)}}\right)I_0\left(\frac{N_na}{K^{(2)}}\right)-K_0\left(\frac{N_na}{K^{(2)}}\right)I_0\left(\frac{N_ns}{K^{(2)}}\right)}\right\}\sin(N_nz) - B_0\frac{(zK_{r2})}{\log_e\left(\frac{s}{a}\right)} + \sum_{q=1}^{Q^I} D_q\left(\frac{rK_{r2}}{K^{(2)}}\right)\left\{\frac{K_0\left(\frac{N_qa}{K^{(2)}}\right)I_1\left(\frac{N_qr}{K^{(2)}}\right)+K_1\left(\frac{N_qr}{K^{(2)}}\right)I_0\left(\frac{N_qa}{K^{(2)}}\right)}{K_0\left(\frac{N_qa}{K^{(2)}}\right)I_0\left(\frac{N_qs}{K^{(2)}}\right)-K_0\left(\frac{N_qs}{K^{(2)}}\right)I_0\left(\frac{N_qa}{K^{(2)}}\right)}\right\} \times \sin(N_qz) - D_0\frac{(zK_{r2})}{\log_e\left(\frac{a}{s}\right)} \tag{47}$$

and

$$\psi_3 = \sum_{p=1}^{P} C_p\left(\frac{rK_{r3}}{K^{(3)}}\right)\left\{\frac{K_0\left(\frac{N_pb}{K^{(3)}}\right)I_1\left(\frac{N_pr}{K^{(3)}}\right)+K_1\left(\frac{N_pr}{K^{(3)}}\right)I_0\left(\frac{N_pb}{K^{(3)}}\right)}{K_0\left(\frac{N_pb}{K^{(3)}}\right)I_0\left(\frac{N_ps}{K^{(3)}}\right)-K_0\left(\frac{N_ps}{K^{(3)}}\right)I_0\left(\frac{N_pb}{K^{(3)}}\right)}\right\}\sin(N_pz) + C_0\frac{(zK_{r3})}{\log_e\left(\frac{b}{s}\right)}, \tag{48}$$

where the constants of integration in Eqs. (46)–(48) are conveniently taken to be zero as we are interested in the difference in value in between any two streamlines rather than their absolute values. For clarity of presentation, the stream functions are generally first normalized before being used for plotting. In normalized form, Eqs. (46)–(48) may be expressed as

$$\psi_1^n(r,z) = \frac{\psi_3(b,h)-|\psi_1(r,z)|}{\psi_3(b,h)}, \tag{49}$$

$$\psi_2^n(r,z) = \frac{\psi_2(r,z)}{\psi_3(b,h)} \tag{50}$$

and

$$\psi_3^n(r,z) = \frac{\psi_3(r,z)}{\psi_3(b,h)}, \tag{51}$$

where the superscript n in the above expressions denotes that these functions are the normalized form of the stream functions related to regions, R-1, R-2 and R-3 of Fig. 1, respectively.

Eqs. (49)–(51) are being used for plotting the normalized streamlines as shown in Fig. 6 for a few flow situations of Fig. 1.

The discharge to the well, Q, can be determined as

$$Q = 2\pi bK_{r3}\int_0^h\left(\frac{\partial\phi_3}{\partial r}\right)_{r=b}dz. \tag{52}$$

Simplification of Eq. (52) yields

$$Q = \frac{2\pi K_{r3}hC_0}{\log_e\left(\frac{b}{s}\right)}. \tag{53}$$

The flow through the sides, Q_s, and bottom, Q_b, of the well can be estimated as

$$Q_s = 2\pi K_{r2}a\int_0^{H_3}\left(\frac{\partial\phi_2}{\partial r}\right)_{r=a}dz \tag{54}$$

and

$$Q_b = 2\pi K_{z1}\int_0^a\left(\frac{\partial\phi_1}{\partial z}\right)_{z=H_3}r\,dr. \tag{55}$$

Eqs. (54) and (55), upon simplification, give

$$Q_s = 2\pi K_{r2}a\left\{\sum_{n=1}^{N} B_n\left[\frac{1}{K^{(2)}}\right]\left[\frac{K_0\left(\frac{N_ns}{K^{(2)}}\right)I_1\left(\frac{N_na}{K^{(2)}}\right)+K_1\left(\frac{N_na}{K^{(2)}}\right)I_0\left(\frac{N_ns}{K^{(2)}}\right)}{K_0\left(\frac{N_ns}{K^{(2)}}\right)I_0\left(\frac{N_na}{K^{(2)}}\right)-K_0\left(\frac{N_na}{K^{(2)}}\right)I_0\left(\frac{N_ns}{K^{(2)}}\right)}\right]\sin(N_nH_3) + \sum_{q=1}^{Q^I} D_q\left[\frac{1}{K^{(2)}}\right]\left[\frac{K_0\left(\frac{N_qa}{K^{(2)}}\right)I_1\left(\frac{N_qa}{K^{(2)}}\right)+K_1\left(\frac{N_qa}{K^{(2)}}\right)I_0\left(\frac{N_qa}{K^{(2)}}\right)}{K_0\left(\frac{N_qa}{K^{(2)}}\right)I_0\left(\frac{N_qs}{K^{(2)}}\right)-K_0\left(\frac{N_qs}{K^{(2)}}\right)I_0\left(\frac{N_qa}{K^{(2)}}\right)}\right]\sin(N_qH_3) - \left(\frac{B_0}{a}\right)\frac{(H_3)}{\log_e\left(\frac{s}{a}\right)} - \left(\frac{D_0}{a}\right)\frac{(H_3)}{\log_e\left(\frac{a}{s}\right)}\right\} \tag{56}$$

and

$$Q_b = -2\pi K_{z1}K^{(1)}a\sum_{m=1}^{M} A_m\frac{I_1\left(\frac{-N_ma}{K^{(1)}}\right)}{I_0\left(\frac{-N_ma}{K^{(1)}}\right)}. \tag{57}$$

3. Verification of proposed model and discussion

In order to check the accuracy of our analytical procedure, we first compare a few results obtained from our proposed solution

with corresponding values obtained from the analytical works of Kirkham [21] and Barua and Hoffmann [1]. It should be noted that the skin zone well hydraulics problem considered here can be reduced to the classical steady state well hydraulics problem [1,21] for a confined aquifer by just assuming the horizontal and vertical hydraulic conductivities of the skin and formation zones to be the same (i.e., $K_{r1} = K_{r2} = K_{r3} = K_{z1} = K_{z2} = K_{z3} = K$). Thus, under this condition, predictions obtained from Kirkham's solution [21] as well as those obtained from Barua and Hoffmann's well hydraulics solution [1] should match with corresponding predictions obtained from the proposed analytical model here. To check the veracity of this, we compare the $Q/Kh(h_a - h_0)$ ratios obtained from our proposed model for a few flow situations of Fig. 1 with corresponding values obtained from Kirkham's solution [21]. Fig. 2 shows such a comparison. As expected, the $Q/Kh(h_a - h_0)$ ratios, as predicted by our analytical model, are found to match very closely with corresponding values obtained from the analytical works of Kirkham (see Table 4 and Fig. 2 of [21]) and Barua and Hoffmann (see Table 2 of [1]), thereby showing the correctness of our developed solution. We would like to point out here that we have expanded only eight terms of our series solution to get the $Q/Kh(h_a - h_0)$ values as the corresponding ratios provided by Kirkham [21] and Barua and Hoffmann [1] were also obtained by expanding only eight terms of his series solution. However, even with expansions carried out only up to eight terms, both these models are seen to predict results which are very close to the corresponding values obtained using the proposed solution.

As a further check to our analytical solution, we next performed a MODFLOW verification of our analytical model for a specific flow geometry of Fig. 1 using Processing Modflow (PMWIN [12]). A PMWIN model was developed, as in Barua and Hoffmann [2], by simulating an 8 m by 8 m confined aquifer of 1 m thickness with a grid network comprising of 80 rows, 80 columns and 20 layers. Thus, the size of the grids considered for modeling was 0.1 m × 0.1 m and the thickness of each layer 0.05 m. To represent approximately a circular well of 0.2 m diameter, further refinements of grids were done in the four centrally located square cells and a constant head of 0.2 m ($h_0 = 0.2$ m) was given to these cells. These well cells were then copied down to the first 10th layer to achieve a partial penetration of 0.45 m of the well in an aquifer of overall thickness 0.9 m. The outer boundary cells (first and the 80th rows and first and the 80th columns) of all the layers were given a constant head of 1.8 m ($h_a = 1.8$ m) and the imperviousness of the top layer (first layer) was achieved by making all the cells of the first layer ineffective except the well cells and the cells in the outer boundaries. Similarly, imperviousness in the bottom layer (20th layer) was modeled by making all the cells of that layer ineffective except the boundary cells where, as mentioned before, a constant head of 1.8 m was provided. For simplicity, we considered the zones R-1, R-2 and R-3 of Fig. 1 to be homogeneous and isotropic within each zone; further, we assumed the hydraulic properties of R-1 and R-2 to be the same in our model. This lumped zone (comprising of R-1 and R-2) was then mimicked by drawing a hydraulic conductivity contrast between a square region of 0.5 m around the well (a four grid sized square domain around the well face up to the penetrating depth of the well and a five grid sized domain below the well depth) and the formation zone. With the above inputs, a steady state PMWIN run was performed for two cases, viz., $K_f/K_s = 1/1$ and $K_f/K_s = 2/1$ (where $K_{r3} = K_{z3} = K_f$ and $K_{r1} = K_{z1} = K_{r2} = K_{z2} = K_s$, and the generated hydraulic heads compared (Tables 1 and 2) with the corresponding analytical values at a few locations of the flow domain. For ease of computation, we have expanded only eight terms of our analytical solution for comparison purpose; however, even with these few term expansions, as may be observed from Tables 1 and 2, our analytical predictions are found to match fairly well with the corresponding

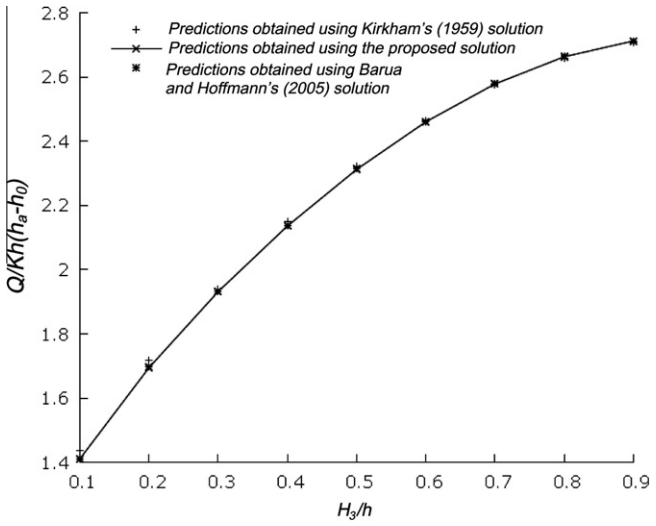

Fig. 2. Comparison of $Q/Kh(h_a - h_0)$ ratios as obtained from the proposed solution for a specific situation of Fig. 1 with the corresponding ratios obtained from the analytical works of Kirkham [21] and Barua and Hoffmann [1] for different H_3/h fractions when the other parameters of the flow configuration are taken as $h/a = 5\pi/4$, $b/a = 10$, $(h_a - h_0)/a = 1$, and $M = N = P = Q^I = 8$.

PMWIN numerical values, thereby proving, once again, the validity of the proposed analytical model. A slight variation among the analytical and numerical hydraulic heads in locations close to the well is understandable because the PMWIN simulations were carried out with an approximately square shaped well rather than a perfectly circular one as has been considered for the analytical development.

We now compare a few of our predictions with corresponding results obtained by Cassiani et al. [6]. Cassiani et al. [6], as mentioned before, obtained a semi-analytical transient solution to the flow problem shown in Fig. 1 by assuming h and $b \to \infty$, a skin of infinitesimal thickness and by neglecting flow through the bottom of the well. Their analysis show that (see Figs. 3–6 of [6]) the dimensionless total flux, $Q_C/\{2\pi K_{2-3} H_3(h_a - h_0)\}$ (where $K_{2-3} = K_{r2} = K_{z2} = K_{r3} = K_{z3}$ and the subscript C in Q_C denotes that the discharge is associated with Cassiani et al.'s theory [6] as distinct from the total discharge symbol Q used in the present paper), for both the skin and no-skin cases, approach quasi-steady states at large times. Similar results were also reported by Chang and Chen [7,8]. The dimensionless total flux plots provided by Cassiani et al. [6] for the quasi-steady situations have given us an opportunity to compare a couple of their no-skin results with our corresponding analytical predictions as the model proposed here, as mentioned before, is also applicable for quasi-steady situations. But for that we must first reduce our solution for the case $K_{r2} = K_{z2} = K_{r3} = K_{z3}$ to the no-bottom-flow condition of Cassiani et al. [6]. In other words, we must make R-1 of Fig. 1 a no flow zone. Also, we must reduce our solution from an aquifer of finite extent to an infinite one, both in the horizontal and vertical directions. The former is equivalent to imposing a no-flow condition $\partial\phi_1/\partial r = 0$ in the boundary $H_3 < z < h$ at $r = s$, and the later is equivalent to making h and b of Fig. 1 very large (theoretically infinite). These conditions can be easily incorporated in our model by simply assigning a very low value (theoretically zero) to K_{r1} and K_{z1} and choosing h and b to be much larger in comparison to other length variables, H_3 and a, of the problem. For $H_3/a = 10$ and $H_3/a = 20$, Cassiani et al.'s [6] $Q_C/\{2\pi K_{2-3} H_3(h_a - h_0)\}$ (in notations of this paper) ratios in the quasi-steady domain turn out to be around 0.37 and 0.29, respectively (see Fig. 3 of [6]; see also Fig. 5 of [8]); thus, for $H_3/a = 10$, we have

$$Q_C = 0.37\{2\pi K_{2-3} H_3(h_a - h_0)\} \tag{58}$$

and, for $H_3/a = 20$, we get

$$Q_C = 0.29\{2\pi K_{2-3} H_3 (h_a - h_0)\} \quad (59)$$

where $h_a - h_0$ can be taken as the drawdown at the well face.

Substituting the values considered for the no-bottom-flow parameters of Fig. 3 ($a = 0.25$ m, $H_3 = 2.5$ m, $K_{2-3} = 20$ m/day; $H_3/a = 10$) and Fig. 4 ($a = 0.125$ m, $H_3 = 2.5$ m, $K_{2-3} = 20$ m/day; $H_3/a = 20$) in Eqs. (58) and (59), respectively, we get, for $H_3/a = 10$

$$Q_C = 116.2389(h_a - h_0) \quad (60)$$

and, for $H_3/a = 20$

$$Q_C = 91.1062(h_a - h_0), \quad (61)$$

where Q_C in Eqs. (60) and (61) is now expressed in m^3/day. Considering a typical drawdown value of 1 (i.e., $h_a - h_0 = 1$) in Eq. (60), we find $Q_C = 116.2389$ m^3/day. Now taking the same values of the no-bottom-flow parameters of Fig. 3 and assuming $h = 10$ m ($H_3/h = 0.25$) and $h_a - h_0 = 1$, we next explore using our developed discharge expression [Eq. (53)] whether a value of b exists to generate the same discharge (i.e., $Q_C = 116.2389$ m^3/day) as has been predicted by Eq. (60); by trial and error using Eq. (53), we find that such a b indeed exists and works out to be 15.43926 m for the considered flow configuration. With the b thus determined, we next generate a discharge-drawdown curve for the flow geometry of Fig. 3 and compare it with the identical curve derived using Cassiani et al.'s [6] Eq. (60). As can be seen in Fig. 3, our predicted curve matches very closely with the one obtained using Eq. (60) for the no-bottom-flow condition. A similar exercise performed for the flow geometry of Fig. 4 ($H_3/a = 20$) yields a b value of 20.29805 m and again the generated discharge-drawdown curve obtained utilizing this b can be seen to be matching very closely with the corresponding curve obtained using Eq. (61), thereby proving, once again, the accuracy of the developed model. As Cassiani et al. [6] validated their theory for the situation $H_3/a = 10$ by comparing dimensionless total flux at the well screen with identical results obtained from the finite difference algorithm of Ruud and Kabala [34] for both transient and quasi-steady situations (see Fig. 3 of [6]), the matching of our quasi-steady discharge values with corresponding values obtained using Cassiani et al.'s solution [6] also, in a way, numerically validates our model.

If we now include bottom flow also in our analysis for the flow geometries of Figs. 3 and 4, respectively, the discharge–drawdown curves, expectedly, shift upward and the difference between bottom-flow and no-bottom-flow discharge values are seen to progressively increase with the increase of drawdown at the well face. To highlight further the importance of bottom flow and the distance of the outer zone b on the overall hydraulics of the problem, we next sought to see the variation of dimensionless total flux, $Q/\{2\pi K_{2-3} H_3 (h_a - h_0)\}$, with b/a for a few flow situations of Fig. 1 for both no-bottom-flow and bottom-flow conditions – Fig. 5 shows the relevant curves. As may be observed from this figure, other things remaining constant, the dimensionless total flux is found to decrease initially rapidly and then less rapidly with the increase of b/a for both no-bottom-flow and bottom-flow conditions, emphasizing the fact that both bottom flow and b play a pivotal role in deciding seepage to a partially penetrating well in a confined aquifer. Thus, these variables are important and hence must be incorporated in the theoretical analysis of the problem. We would like to point out here that Chang and Chen [8] found that if the thickness of an aquifer exceeds more than 100 times the screen length (i.e., $h/H_3 > 100$),the aquifer can be considered a semi-infinite one in the vertical direction for times of practical significance and that Cassiani et al.'s model [6] in that case is applicable (see Fig. 5 of [8]). We have, however, seen here that for an aquifer of finite horizontal and vertical extent, the requirement of $h/H_3 > 100$ for an aquifer to be considered semi-infinite in the vertical plane, need not always be necessary provided the horizontal extent of the aquifer is also considered for analysis; in fact, for the flow geometries of Figs. 3 and 4, respectively, we could generate the quasi-steady discharge-drawdown curves of Cassiani et al. [6] by considering $h/H_3 = 4$ only provided the outer zone b is placed at a distance of 15.43926 m for$H_3/a = 10$ and 20.29805 m for $H_3/a = 20$, from the centre of the well.

Fig. 6 shows normalized streamlines for a few flow situations of Fig. 1. It can be observed from the figure that the slopes of the streamlines get changed at the common boundary for both positive and negative skins and as one moves from the formation to the skin zone, the slopes decrease for positive ($K_f/K_s = 5/1$) and increase for negative skin ($K_f/K_s = 1/5$), thereby showing that the hydraulic conductivity contrast between the skin and formation zones plays

Table 1
Differences of analytically predicted and numerically obtained hydraulic heads at a few coordinates of the flow domain of Fig. 1 when the parameters of the flow configuration are taken as $h = 0.90$ m, $H_3 = 0.45$ m, $a = 0.10$ m, $s = 0.50$ m, $b = 3.90$ m, $h_a = 1.80$ m, $h_0 = 0.20$ m and $K_f/K_s = 1/1$.

Vertical distance, z (m)	Radial distance, r (m)				
	0.30 Anal. – Num. (m)	0.60 Anal. – Num. (m)	0.90 Anal. – Num. (m)	1.20 Anal. – Num. (m)	1.50 Anal. – Num. (m)
0.25	0.0702	0.0091	0.0081	0.0109	0.0136
0.50	0.0607	0.0137	0.0093	0.0110	0.0137
0.75	0.0076	0.0076	0.0085	0.0110	0.0137

Num.: Hydraulic heads obtained by numerical means (PMWIN).
Anal.: Hydraulic heads obtained from the developed theory.

Table 2
Differences of analytically predicted and numerically obtained hydraulic heads at a few coordinates of the flow domain of Fig. 1 when the parameters of the flow configuration are taken as $h = 0.90$ m, $H_3 = 0.45$ m, $a = 0.10$ m, $s = 0.50$ m, $b = 3.90$ m, $h_a = 1.80$ m, $h_0 = 0.20$ m and $K_f/K_s = 2/1$.

Vertical distance, z (m)	Radial distance, r (m)				
	0.30 Anal. – Num. (m)	0.60 Anal. – Num. (m)	0.90 Anal. – Num. (m)	1.20 Anal. – Num. (m)	1.50 Anal. – Num. (m)
0.25	0.0761	−0.0011	−0.0014	0.0011	0.0039
0.50	0.0518	−0.0020	−0.0017	0.0010	0.0038
0.75	−0.0016	−0.0075	−0.0030	0.0006	0.0038

Num.: Hydraulic heads obtained by numerical means (PMWIN).
Anal.: Hydraulic heads obtained from the developed theory.

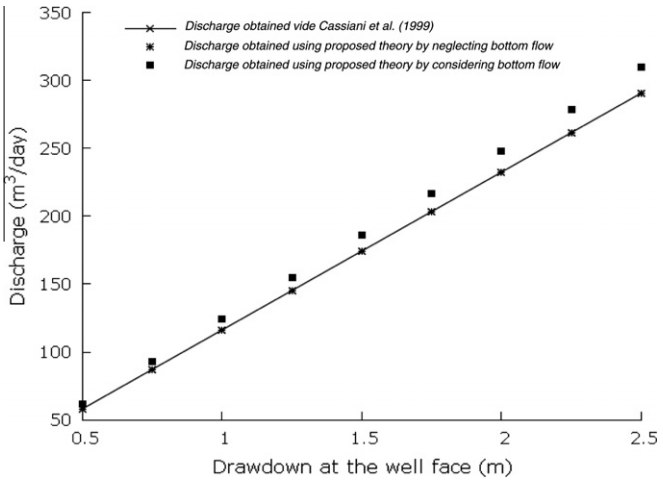

Fig. 3. Comparison of discharge–drawdown curves as obtained from the proposed solution of Fig. 1 with the corresponding curves obtained from Cassiani et al.'s [6] solution when the flow parameters of Fig. 1 are taken as $h = 10.00$ m, $H_3 = 2.50$ m, $a = 0.25$ m, $b = 15.43926$ m and (a) $K_{r1} = K_{z1} = 0.00001$ m/day and $K_{2-3} = 20$ m/day for the no-bottom-flow and (b) $K_{r1} = K_{z1} = K_{2-3} = 20$ m/day for the bottom-flow conditions.

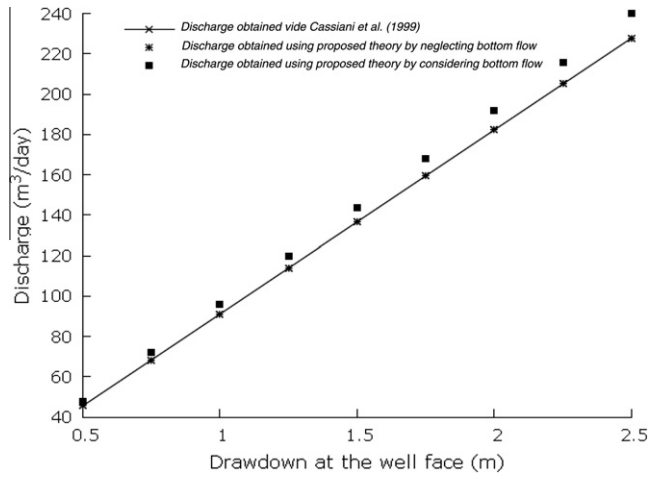

Fig. 4. Comparison of discharge–drawdown curves as obtained from the proposed solution of Fig. 1 with the corresponding curves obtained from Cassiani et al.'s [6] solution when the flow parameters of Fig. 1 are taken as $h = 10.00$ m, $H_3 = 2.50$ m, $a = 0.125$ m, $b = 20.29805$ m and (a) $K_{r1} = K_{z1} = 0.00001$ m/day and $K_{2-3} = 20$ m/day for the no-bottom-flow and (b) $K_{r1} = K_{z1} = K_{2-3} = 20$ m/day for the bottom-flow conditions.

an important part in deciding flow to a well in a confined aquifer. It should further be noted that, for the flow geometries considered, bottom flow accounts for nearly 20% of the overall flow to the well for the negative skin situation and that this fraction tends to increase with the decrease in K_f/K_s ratio. Thus, among other factors remaining constant, neglecting bottom flow to a partially penetrating well in a confined aquifer may induce large error in discharge values, particularly for situations where the K_f/K_s ratio is low.

4. Inverse modeling and field applications

We now perform an inverse modeling utilizing our proposed model to estimate s, K_f and K_s using field results obtained from a typical pumping test in a confined aquifer. Actually, the inverse modeling can be carried out to estimate any desired parameter(s) of Fig. 1; however, for simplicity, we are here localizing our attention to the parameters s, K_f and K_s only. In other words, in our simulation here, we assume the geometry of the well and the aquifer extent, both in the horizontal and vertical directions, to be fully known, regions R-1, R-2 and R-3 of Fig. 1 to be homogeneous and isotropic within each zone and the conductivity of R-1 and R-2 to be the same. The horizontal extent b at any instant of time in the quasi-steady pumping state may be assumed to be simply the distance of a relatively faraway piezometer from the centre of the well, with the corresponding h_a equaling with the head sensed by the said piezometer at that instant. This is because, the streamlines at faraway locations from the centre of a pumping well will be almost horizontal and the vertical component of the velocity vector in those locations will be almost negligible (Fig. 6). Naturally, the error induced due to this assumption will decrease with the increase of distance of a piezometer location from the centre of the well. Proceeding in the usual way, the function to be minimized, $F_m(s,\theta)$, can be expressed as a sum of the square of the difference between the predicted and the observed hydraulic heads at different piezometric locations – the resultant expression works out to be

$$F_m(s,\theta) = \sum_{i=1}^{N_{pz}} \{\phi_p(r_i,z_i) - \phi_o(r_i z_i)\}^2, \tag{62}$$

where $\phi_p(r_i,z_i)$ and $\phi_o(r_i,z_i)$ are the predicted and observed hydraulic heads at the (r_i,z_i)th location, $\theta = K_f/K_s$ and N_{pz} is the number of piezometric locations. Minimizing the function in Eq. (62) with respect to s and θ, we get

$$\sum_{i=1}^{N_{pz}} \{\phi_p(r_i,z_i) - \phi_o(r_i,z_i)\} \frac{\partial \phi_p(r_i,z_i)}{\partial s} = 0 \tag{63}$$

and

$$\sum_{i=1}^{N_{pz}} \{\phi_p(r_i,z_i) - \phi_o(r_i,z_i)\} \frac{\partial \phi_p(r_i,z_i)}{\partial \theta} = 0, \tag{64}$$

where $\phi_p(r_i,z_i)$, $\partial\phi_p(r_i,z_i)/\partial s$ and $\partial\phi_p(r_i,z_i)/\partial\theta$ can be determined at the (r_i,z_i)th location from our relevant hydraulic head expressions given in Eqs. (3) and (4), respectively, and $\phi_o(r_i,z_i)$ is the observed hydraulic head at that location. Eqs. (63) and (64) can now be solved by running a Newton–Raphson (N–R) procedure [36] and s and θ, thus, can be evaluated. Once s and θ are being determined and knowing the pumping rate, the hydraulic conductivities of the

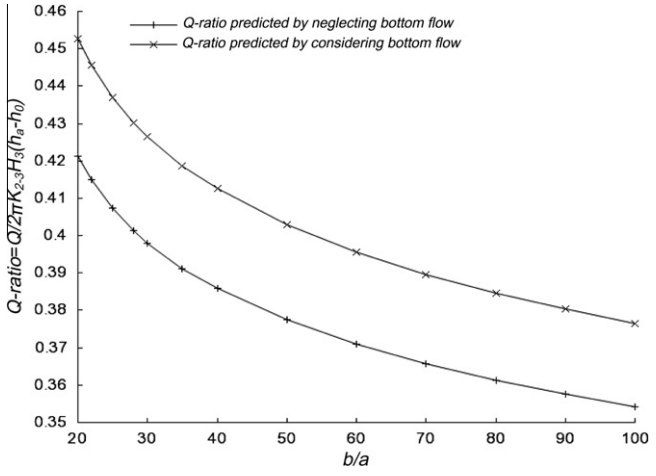

Fig. 5. Variation of $Q/2\pi K_{2-3}H_3(h_a - h_0)$ with b/a ratios for a few flow situations of Fig. 1 when the other flow parameters of the problem are taken as $H_3/h = 0.25$, $H_3/a = 10.00$, $(h_a - h_0) = 1.00$ m and (a) $K_{r1} = K_{z1} = 0.00001$ m/day and $K_{2-3} = 20$ m/day for the no-bottom-flow and (b) $K_{r1} = K_{z1} = K_{2-3} = 20$ m/day for the bottom-flow conditions.

formation and skin zones can next be calculated using the discharge expression given in Eq. (53).

The computational effort involved in the inverse modeling can be considerably reduced if we apply Eqs. (63) and (64) to ϕ_3 only, considering only those piezometer readings lying on or outside the assumed skin zone thickness s, and not to both ϕ_2 and ϕ_3 at the same time involving piezometer readings of both regions R-2 and R-3, respectively. With the s and θ thus estimated in a run, Eq. (62) is next applied, using ϕ_2, to work out the sum of the square of the difference between the predicted and observed hydraulic heads taking now the piezometer readings of R-2 alone – the idea is to determine a pair of s and θ, which will make this difference as small as possible and at the same time satisfy Eqs. (63) and (64) (with ϕ_3) as closely as possible. Of course, with a single run, the evaluated s and θ may not yield the desired result but, by trial and error, a pretty accurate estimate of s and θ may be made, particularly for situations where the skin zone is of a much smaller thickness as compared to the thickness of the formation zone.

Now, with our inverse modeling assumptions, ϕ_3 can be expressed as

$$\phi_3 = \sum_{p=1}^{P} C_p \left\{ \frac{K_0(N_p b) I_0(N_p r) - K_0(N_p r) I_0(N_p b)}{K_0(N_p b) I_0(N_p s) - K_0(N_p s) I_0(N_p b)} \right\} \cos(N_p z) - C_0 \frac{\log_e\left(\frac{b}{r}\right)}{\log_e\left(\frac{b}{s}\right)} + h_a. \tag{65}$$

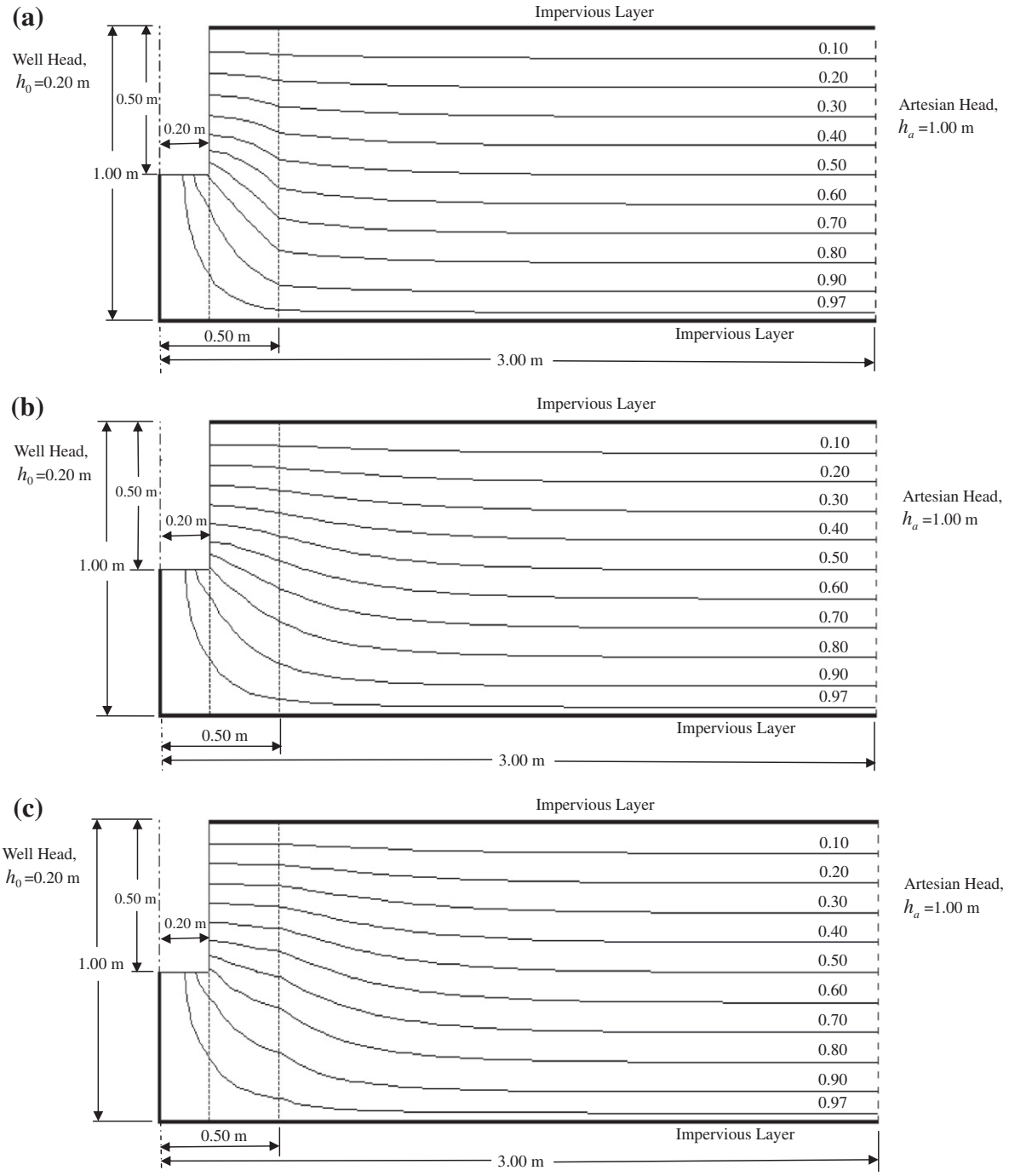

Fig. 6. Normalized streamlines corresponding to Fig. 1 when the flow geometries are as shown: (a) $K_f/K_s = 1/5$; (b) $K_f/K_s = 1/1$; (c) $K_f/K_s = 5/1$.

The s-derivative of ϕ_3 in Eq. (63) then turns out to be

$$\frac{\partial\phi_3}{\partial s} = -\sum_{p=1}^{P} C_p(N_p)\left\{\frac{K_0(N_pb)I_0(N_pr) - K_0(N_pr)I_0(N_pb)}{[K_0(N_pb)I_0(N_ps) - K_0(N_ps)I_0(N_pb)]^2}\right\} \times \{K_0(N_pb)I_1(N_ps) + K_1(N_ps)I_0(N_pb)\}\cos(N_pz) - C_0\left\{\left(\frac{1}{s}\right)\frac{\log_e\left(\frac{b}{r}\right)}{\left[\log_e\left(\frac{b}{s}\right)\right]^2}\right\}. \quad (66)$$

To evaluate the θ – derivative of ϕ_3 for Eq. (64), we must first bring θ into the expression for ϕ_3; this can be done by simply incorporating C_0 [Eq. (20)] into Eq. (65) – ϕ_3 can then be expressed as

$$\phi_3 = \sum_{p=1}^{P} C_p\left\{\frac{K_0(N_pb)I_0(N_pr) - K_0(N_pr)I_0(N_pb)}{K_0(N_pb)I_0(N_ps) - K_0(N_ps)I_0(N_pb)}\right\}\cos(N_pz) + \left\{\frac{\frac{h_a}{\log_e\left(\frac{a}{s}\right)} + \frac{B_0}{\log_e\left(\frac{s}{a}\right)}}{\frac{\theta}{\log_e\left(\frac{b}{s}\right)} - \frac{1}{\log_e\left(\frac{a}{s}\right)}}\right\}\frac{\log_e\left(\frac{b}{r}\right)}{\log_e\left(\frac{b}{s}\right)} + h_a. \quad (67)$$

Differentiating Eq. (67) with respect to θ, we get

$$\frac{\partial\phi_3}{\partial\theta} = -\left\{\frac{1}{\log_e\left(\frac{b}{s}\right)}\right\}\left\{\frac{\frac{h_a}{\log_e\left(\frac{a}{s}\right)} + \frac{B_0}{\log_e\left(\frac{s}{a}\right)}}{\left[\frac{\theta}{\log_e\left(\frac{b}{s}\right)} - \frac{1}{\log_e\left(\frac{a}{s}\right)}\right]^2}\right\}\left\{\frac{\log_e\left(\frac{b}{r}\right)}{\log_e\left(\frac{b}{s}\right)}\right\}. \quad (68)$$

Eqs. (63) and (64) can now be solved by making use of Eqs. (66) and (68), respectively, in the simplified inverse modeling approach. We would like to point here that the method just mentioned is an approximate one where the N–R is actually applied to only piezometer readings falling in the formation zone. However, the method is found to work very well (see Section 4.1) for situations, as mentioned before, where the thickness of the skin zone is considerably less as compared to that of the formation zone. Moreover, the approximate method also serves quite well to make, at least, a rough estimate of the parameters s and θ, which in turn can then be used as initial inputs in the N–R for the inverse modeling performed with both ϕ_2 and ϕ_3 combined. We now present an example of the approximate method using quasi-steady pumping test data of 'Oude Korendijk', the Netherlands [22].

4.1. Example

A pumping test was performed in 'Oude Korendijk' [22] on a fully penetrating confined aquifer of thickness 7 m with a constant discharge of 788 m^3/day. It was observed that the water levels in the piezometers, located at radial distances of 30 m and 90 m, respectively, from the centre of the well, had not stabilized even after 830 min of pumping but a quasi-steady state was reached only after 10 min of pumping. The quasi-steady drawdowns, s_w, observed on these piezometers at the end of 18 min of pumping were (see Table 3.1 of [22]): $s_w(30,2) = 0.6800$ m and $s_w(90,6) = 0.3050$ m, respectively, where the z-coordinates of the piezometer locations indicate that the 30 and 90 piezometers were installed at depths of 2 m and 6 m, respectively, from the top confining stratum.

The average transmissivity of the aquifer obtained using Thiem's method [22] works out to be 385 m^2/day (Kb); we assume the same value here. Further, we assume the radius of the well to be 0.1 m for all computations as this information was not provided in the pumping test data. Now the steady/quasi-steady discharge, Q_T, for a homogeneous and isotropic confined aquifer can be expressed as (Thiem's equation)

$$Q_T = 2\pi Kb\left\{\frac{s_w(r_1) - s_w(r_2)}{\log_e(r_2/r_1)}\right\}, \quad (69)$$

where $s_w(r_1)$ and $s_w(r_2)$ are the drawdowns on piezometers located at radial distances r_1 and r_2, respectively, from the centre well, and the other symbols have already been defined. It should be noted that Eq. (69) is developed by assuming the flow to be only radial (i.e., neglecting vertical flow) and as such is an approximate expression. However, because of its simplicity, the expression allows a very easy way of roughly estimating the well face drawdown and the associated radius of influence corresponding to a steady/quasi-steady situation, provided the drawdown information at known piezometeric location(s), transmissivity of the aquifer and the radius of the pumping well are known. Applying Eq. (69) to the 18-min drawdown data of the 30 m piezometer, we get, $h_a - h_0 = 2.5380$ m and $b = 241.9381$ m; a similar application to the drawdown data of the 90 m piezometer yields $h_a - h_0 = 2.5208$ m and $b = 229.5470$ m. Thus, the average quasi-steady $h_a - h_0$ and b at the end of 18 min of pumping can be approximately taken as 2.5294 m and 235.7426 m, respectively. Taking $h_a - h_0 = 2.5294$ m and using Eq. (69), we next generate 18-min approximate drawdowns for two piezometers located, say, at distances of 0.8 m and 60 m, respectively, from the centre of the well – the resultant drawdowns work out to be 1.8520 m and 0.4456 m, respectively. Assuming further that these piezometers are installed at a depth of 6 m and 4 m, respectively, from the base of the top confining stratum, we have $s_w(0.8,6) = 1.8520$ m, and $s_w(60,4) = 0.4456$ m. Reducing the drawdowns to the corresponding hydraulic heads and assuming the 0.8 m piezometer to be located in the skin zone, we have $\phi_2(0.8,6) = 0.6774$ m, $\phi_3(30,2) = 1.8494$ m, $\phi_3(60,4) = 2.0838$ m and $\phi_3(90,6) = 2.2244$ m. We have now come to a stage where we have obtained all the necessary data for our inverse modeling except that we are yet to assign any value to H_3. But as the 'Oude Korendijk' [22] well was a fully penetrating one, H_3 can be given any value as long as it is very close to h; we take $H_3 = 6.95$ m here. With the above inputs and considering only six terms of our series solution, an inversemodeling has been performed which yields $s = 16.2612$ m, $\theta = K_f/K_s = 0.9934$, $K_f = 54.7106$ m/day and $K_s = 55.0760$ m/day. At this stage, the left-hand-sides of Eqs. (63) and (64) have been observed to be 1.0×10^{-10} and 0.1726×10^{-10}, respectively, and the sum of the square of the difference between predicted and observed heads for the skin zone piezometer as 7.2276×10^{-09}. Thus, it may concluded that the 'Oude Korendijk' [22] aquifer is a fairly homogeneous one with an average transmissivity of 384.2531 m^2/day $[(54.7106 + 55.0760) \times 7 \times 0.5]$, a value very close to 385 m^2/day, obtained using Thiem's equation. We would like to point out here that we could perform successfully our inverse modeling procedure here by considering only 18-min quasi-steady drawdown data of the 'Oude Korendijk' [22] pumping test. This shows that the model proposed here can very well be adopted for analyzing short-time drawdown data as well, provided, of course, the data fall in the quasi-steady domain of a typical pumping test. This is an important observation because a considerable pumping time may be required for an artesian aquifer to come to steady state but a quasi-steady may be reached on a relatively much shorter time [22]. For example, in case of the 'Oude Korendijk' test, the drawdowns on the 30 m and 90 piezometers were observed to exhibit quasi-steady behavior only after 10 min of pumping whereas the steady state was not reached even after 830 min of pumping [22].

For the same well geometry and the well discharge, let us now consider a hypothetical situation where the quasi-steady hydraulic heads at a couple of piezometers around the well are, say, $\phi_2(0.8,1) = 0.4200$ m, $\phi_2(2,3) = 0.6050$ m, $\phi_2(4,5) = 0.7450$ m, $\phi_3(10,1) = 1.0700$ m, $\phi_3(30,2) = 1.5140$ m, $\phi_3(50,3) = 1.7200$ m, $\phi_3(70,4) = 1.8560$ m and $\phi_3(90,5) = 1.9570$ m, where we have assumed the skin zone to extend beyond 4 m. For the above flow situation, let the corresponding b be 100 m. Now, carrying out an inverse simulation as before by expanding only up to eight terms of our series solution, we get $s = 4.9918$ m, $\theta = K_f/K_s = 0.4995$, $K_f = 44.2999$ m/day and $K_s = 88.6911$ m/day. At this stage, the

left-hand-sides of Eqs. (63) and (64) have been observed to be 0.0051×10^{-8} and 0.1388×10^{-8}, respectively, and the sum of the square of error for the skin zone piezometer as 5.9231×10^{-8}.

5. Conclusions

The hydraulic head function, and from it the stream function and the flow rate, have been derived for groundwater seeping into a partially penetrating well in an artesian aquifer with skin zone and underlain by an impervious layer. The proposed solution accounts for bottom flow, non-uniform flow at the well face, finite skin thickness and finite horizontal and vertical extent of an artesian aquifer and can also be reduced to incorporate the mixed-type boundary condition at the well face. The validity of the proposed model has been tested by comparing our results with identical results obtained from the analytical works of Kirkham [21], Cassiani et al. [6] and Barua and Hoffmann [1] for a few specific flow situations of Fig. 1. Further, a numerical check on the proposed model has also been done by comparing our model predictions with corresponding results obtained from PMWIN [12], again for a few flow situations of Fig. 1. An inverse modeling has been performed, using the developed analytical solution, to estimate skin thickness and conductivities of the skin and formation zones of a patchy confined aquifer by utilizing results obtained from a standard pumping test. The study shows that the conductivity contrast and thickness of the skin and formation zones, bottom flow and horizontal and vertical extent of an artesian aquifer play an important part in the overall hydraulics of the skin hydraulics problem and hence these factors must be considered while analyzing the problem. It is also observed that the positive skin has a tendency to flatten the streamlines and that the negative skin has a tendency to straighten them up as one moves from the formation to the skin zone. Further, among other factors remaining constant, bottom flow may account for a sizeable portion of the total flow particularly for situations where the conductivity ratio between the formation and skin zones is considerably low. It is hoped that proposed model will be of use in analyzing flow behavior around a pumping well in an artesian aquifer underlain by an impervious layer, particularly for situations where the hydraulic properties of the aquifer in the immediate neighborhood of the well are found to differ from locations farther away from the well.

Acknowledgement

This work forms a part of DST (Department of Science and Technology, Government of India) Project No. SR/S4/ES-123/2004. We are thankful to the DST for providing the necessary financial support to carryout the project.

Appendix. Determination of hydraulic head functions

In this section, we provide general expressions for the hydraulic head functions corresponding to regions R-1, R-2 and R-3 of Fig. 1. We proceed by first obtaining a set of solutions to Eq. (1) using the separation of variable method.

Dropping the indices and substituting $(K_0')^2 = K_r/K_z$ in Eq. (1) and simplifying, we get

$$(K_0')^2 \frac{\partial^2 \phi}{\partial r^2} + (K_0')^2 \frac{1}{r}\frac{\partial \phi}{\partial r} + \frac{\partial^2 \phi}{\partial z^2} = 0. \tag{A1}$$

Let

$$\phi = R(r)Z(z), \tag{A2}$$

be a solution of Eq. (A1), where $R(r)$ and $Z(z)$ are functions of r and z, respectively. Applying Eq. (A2) to (A1) and separating the variables out, we find the resultant expression as

$$(K_0')^2 \frac{R''(r)}{R(r)} + (K_0')^2 \frac{1}{r}\frac{R'(r)}{R(r)} = -\frac{Z''(z)}{Z(z)}. \tag{A3}$$

An inspection of Eq. (A3) shows that both the right-hand and left-hand sides of the above equation can be equated to a constant – let it be α^2, where we first take $\alpha^2 > 0$. The ensuing equations obtained by equating Eq. (A3) to α^2 can be written as

$$Z''(z) + \alpha^2 Z(z) = 0, \tag{A4}$$

and

$$r^2 R''(r) + rR'(r) - \left\{\frac{r\alpha}{(K_0')}\right\}^2 R(r) = 0. \tag{A5}$$

A solution of Eq. (A4) can be expressed as

$$Z(z) = E\sin(\alpha z) + F\cos(\alpha z), \tag{A6}$$

and a solution of Eq. (A5) is

$$R(r) = GI_0\left(\frac{\alpha r}{K_0'}\right) + HK_0\left(\frac{\alpha r}{K_0'}\right), \tag{A7}$$

where E, F, G and H are any arbitrary constants and $I_0(\cdot)$ and $K_0(\cdot)$ are zero order modified Bessel functions of first and second kinds, respectively. Of course, $Z(z)$ by considering only the sine or the cosine term of Eq. (A6) will still be a solution of Eq. (A4). Similarly, $R(r)$ with either one of the Bessel functions of Eq. (A7) will also be a solution of Eq. (A5). Substituting $R(r)$ and $Z(z)$ of Eqs. (A6) and (A7) in Eq. (A2), we find

$$\phi = \left\{GI_0\left(\frac{\alpha r}{K_0'}\right) + HK_0\left(\frac{\alpha r}{K_0'}\right)\right\}\{E\sin(\alpha z) + F\cos(\alpha z)\}, \tag{A8}$$

as one of the solutions of the governing differential equation (A1). Now, considering $\alpha^2 = 0$, and noting the fact that any arbitrary constant is also a solution of Eq. (A1), we see that

$$\phi = L\log_e(M/r), \tag{A9}$$

is an another solution of Eq. (A1), where L and M are any arbitrary constants. Since the sum of solutions of a differential equation is also its solution, a general solution of Eq. (A1) can thus be written as

$$\phi = \sum_{n=1}^{N_0}\left\{G_n I_0\left(\frac{\alpha_n r}{K_0'}\right) + H_n K_0\left(\frac{\alpha_n r}{K_0'}\right)\right\}\{E_n\sin(\alpha_n z) + F_n\cos(\alpha_n z)\} + R\log_e\left(\frac{S}{r}\right) + T, \tag{A10}$$

where E_n, F_n, G_n, H_n, R, S and T are all arbitrary constants. Further, as mentioned before, a hydraulic head expression obtained from the above by dropping a trigonometric or a Bessel function or a combination of both a trigonometric and a Bessel function, will still be a solution of Eq. (1).

In view of the above, the hydraulic head expressions ϕ_1, ϕ_2 and ϕ_3 corresponding to regions R-1, R-2 and R-3 of Fig. 1 may be expressed as

$$\phi_1 = \sum_{m=1}^{M} A_m \frac{I_0\left\{\frac{-(1-2m)\pi r}{2K^{(1)}(h-H_3)}\right\}}{I_0\left\{\frac{-(1-2m)\pi a}{2K^{(1)}(h-H_3)}\right\}}\sin\left\{\frac{(1-2m)\pi(z-H_3)}{2(h-H_3)}\right\} + h_0, \tag{A11}$$

$$\phi_2 = \sum_{n=1}^{N} B_n\left\{\frac{K_0\left(\frac{n\pi s}{K^{(2)}h}\right)I_0\left(\frac{n\pi r}{K^{(2)}h}\right) - K_0\left(\frac{n\pi r}{K^{(2)}h}\right)I_0\left(\frac{n\pi s}{K^{(2)}h}\right)}{K_0\left(\frac{n\pi s}{K^{(2)}h}\right)I_0\left(\frac{n\pi a}{K^{(2)}h}\right) - K_0\left(\frac{n\pi a}{K^{(2)}h}\right)I_0\left(\frac{n\pi s}{K^{(2)}h}\right)}\right\}\cos\left(\frac{n\pi z}{h}\right) + B_0\frac{\log_e\left(\frac{s}{r}\right)}{\log_e\left(\frac{s}{a}\right)} + \sum_{q=1}^{Q'} D_q\left\{\frac{K_0\left(\frac{q\pi a}{K^{(2)}h}\right)I_0\left(\frac{q\pi r}{K^{(2)}h}\right) - K_0\left(\frac{q\pi r}{K^{(2)}h}\right)I_0\left(\frac{n\pi a}{K^{(2)}h}\right)}{K_0\left(\frac{q\pi a}{K^{(2)}h}\right)I_0\left(\frac{q\pi s}{K^{(2)}h}\right) - K_0\left(\frac{q\pi s}{K^{(2)}h}\right)I_0\left(\frac{q\pi a}{K^{(2)}h}\right)}\right\} \times \cos\left(\frac{q\pi z}{h}\right) + D_0\frac{\log_e\left(\frac{a}{r}\right)}{\log_e\left(\frac{a}{s}\right)} \tag{A12}$$

and

$$\phi_3 = \sum_{p=1}^{P} C_p \left\{ \frac{K_0\left(\frac{p\pi b}{K^{(3)}h}\right) I_0\left(\frac{p\pi r}{K^{(3)}h}\right) - K_0\left(\frac{p\pi r}{K^{(3)}h}\right) I_0\left(\frac{p\pi b}{K^{(3)}h}\right)}{K_0\left(\frac{p\pi b}{K^{(3)}h}\right) I_0\left(\frac{p\pi s}{K^{(3)}h}\right) - K_0\left(\frac{p\pi s}{K^{(3)}h}\right) I_0\left(\frac{p\pi b}{K^{(3)}h}\right)} \right\} \cos\left(\frac{p\pi z}{h}\right) - C_0 \frac{\log_e\left(\frac{b}{r}\right)}{\log_e\left(\frac{b}{s}\right)} + h_a, \tag{A13}$$

where M, N, P and Q are any positive integers, i.e.,

$$M = 1,2,3,\ldots, \quad N = 1,2,3,\ldots, \quad P = 1,2,3,\ldots, \quad Q^I = 1,2,3,\ldots, \tag{A14}$$

$$K^{(i)} = \left(K_{ri}/K_{zi}\right)^{1/2}, \quad i = 1,2,3, \tag{A15}$$

m, n, p and q are summation indices, and A_m, B_n, C_p, D_q, B_0, C_0 and D_0 are constants to be determined from the given boundary and interfacial conditions. It should be noted that Eqs. (A11)–(A13) are formulated in such a way that they inherently satisfy conditions I, II, III, IV, V, VII, VIII, IX of the flow problem considered. We show in the text how the remaining boundary and interfacial conditions can be used to work out the constants appearing in these equations.

References

[1] Barua G, Hoffmann MR. Theory of seepage into an auger hole in a confined aquifer. J Irrig Drain Eng 2005;131(5):440–50.
[2] Barua G, Hoffmann MR. Theory of seepage into an auger hole in a confined aquifer overlying a gravel substratum. J Irrig Drain Eng 2007;133(4):330–41.
[3] Bear J. Dynamics of fluids in porous media. New York: American Elsevier Publishing Company, Inc.; 1972. p. 235.
[4] Butler Jr JJ. Pumping tests in nonuniform aquifers – the radially symmetric case. J Hydrol 1988;101:15–30.
[5] Cassiani G, Kabala ZJ. Hydraulics of a partially penetrating well: solution to a mixed-type boundary value problem via dual integral equations. J Hydrol 1998;211:100–11.
[6] Cassiani G, Kabala ZJ, Medina Jr MA. Flowing partially penetrating well: solution to a mixed-type boundary value problem. Adv Water Resour 1999;23(1):59–68.
[7] Chang CC, Chen CS. An integral transform approach for a mixed boundary problem involving a flowing partially penetrating well with infinitesimal well skin. Water Resour Res 2002;38(6):1071.
[8] Chang CC, Chen CS. A flowing partially penetrating well in a finite-thickness aquifer: a mixed-type initial boundary value problem. J Hydrol 2003;271:101–18.
[9] Chang YC, Yeh HD. New solutions to the constant-head test performed at a partially penetrating well. J Hydrol 2009;369:90–7.
[10] Chang YC, Yeh HD. A new analytical solution solved by triple series equations method for constant head tests in confined aquifers. Adv Water Resour 2010;33:640–51.
[11] Chang YC, Yeh HD, Chen GY. Transient solution for radial two-zone flow in unconfined aquifers under constant-head tests. Hydrol Process 2010;24:1496–503.
[12] Chiang W, Kinzelbach W. 3D-Groundwater modeling with PMWIN: a simulation system for modeling groundwater flow and pollution. Berlin: Springer-Verlag; 2001.
[13] Chiu PY, Yeh HD, Yang SY. A new solution for a partially penetrating constant-rate pumping well with a finite-thickness skin. Int J Numer Anal Meth Geomech 2007;31:1659–74.
[14] Cimen M. Type curves for unsteady flow to a large-diameter well in patchy aquifers. J Hydraul Eng 2005;10(3):200–4.
[15] Dagan G. A note on packer, slug and recovery tests in unconfined aquifers. Water Resour Res 1978;14:929–34.
[16] Dougherty DE, Babu DK. Flow to a partially penetrating well in a double-porosity reservoir. Water Resour Res 1984;20(8):1116–22.
[17] Gringarten AC, Ramey Jr HJ. An approximate infinite conductivity solution for a partially penetrating line-source well. Soc Petrol Eng J 1975;259:140–8.
[18] Hantush MS. Hydraulics of wells. In: Chow VT, editor. Advances in hydroscience, vol. 1. New York: Academic Press; 1964.
[19] Hemker CJ. Transient well flow in vertically heterogeneous aquifers. J Hydrol 1999;225:1–18.
[20] Hyder Z, Butler Jr JJ, McElvee CD, Liu W. Slug tests in partially penetrating wells. Water Resour Res 1994;30(11):2945–57.
[21] Kirkham D. Exact theory of flow into a partially penetrating well. J Geophys Res 1959;64:1317–27.
[22] Kruseman GP, de Ridder NA. Analysis and evaluation of pumping test data. 2nd ed. Wageningen, The Netherlands: International Institute for Land Reclamation and Improvement; 1994. Publication 47, p. 55–61.
[23] Lee TC, Damiata BN. Distortion in resistivity logging as shallow depth. Geophysics 1995;60:1058–69.
[24] Maas C. Groundwater flow to a well in a layered porous medium. 2. Nonsteady multiple-aquifer flow. Water Resour Res 1987;23(8):1683–8.
[25] Moench AF. Transient flow to a large-diameter well in an aquifer with storative semiconfining layers. Water Resour Res 1985;21(8):1121–31.
[26] Neuman SP. Effects of partial penetration on flow in unconfined aquifers considering delayed aquifer response. Water Resour Res 1974;10(2):303–12.
[27] Neuman SP, Guadagnini A, Riva M. Type-curve estimation of statistical heterogeneity. Water Resour Res 2004;40:W04201.
[28] Neuman SP, Blattstein A, Riva M, Tartakovsky DM, Guadagnini A, Ptak T. Type curve interpretation of late-time pumping test data in randomly heterogeneous aquifers. Water Resour Res 2007;43:W10421.
[29] Novakowski KS. A composite analytical model for analysis of pumping tests affected by wellbore storage and finite thickness skin. Water Resour Res 1989;25(9):1937–46.
[30] Novakowski KS. Analysis of aquifer tests conducts in fractured rocks: a review of the physical computer program for generating type curves. Ground Water 1990;28(1):99–107.
[31] Novakowski KS. Interpretation of the transient flow rate obtained from constant-head tests conducted in situ in clays. Can Geotech J 1993;30:600–6.
[32] Pasandi M, Samani N, Barry DA. Effect of wellbore storage and finite thickness skin on flow to a partially penetrating well in a phreatic aquifer. Adv Water Resour 2008;31(2):383–98.
[33] Perina T, Lee TC. General well function for pumping from a confined, leaky, or unconfined aquifer. J Hydrol 2006;317:239–60.
[34] Ruud NC, Kabala ZJ. Numerical evaluation of flowmeter test interpretation methodologies. Water Resour Res 1996;32(4):845–52.
[35] Ruud NC, Kabala ZJ. Response of a partially penetrating well in a heterogeneous aquifer: integrated well-face flux vs. uniform well-face flux boundary conditions. J Hydrol 1997;194:76–94.
[36] Scarborough JB. Numerical mathematical analysis. 6th ed. New Delhi: Oxford and IBH Publishing Company Private Limited; 1966. p. 203–7, 269–96.
[37] Selim MS, Kirkham D. Screen theory for wells and soil drain pipes. Water Resour Res 1974;10(5):1019–30.
[38] Widdowson MA, Molz FJ, Melville JG. An analysis technique for multilevel and partially penetrating slug test data. Ground Water 1990;28(6):937–45.
[39] Yang SY, Yeh HD. Solution for flow rates across the wellbore in a two-zone confined aquifer. J Hydraul Eng 2002;128(2):175–83.
[40] Yang SY, Yeh HD. A simple approach using Bouwer and Rice's method for slug test data analysis. Ground Water 2004;42(5):781–4.
[41] Yang SY, Yeh HD. Laplace-domain solutions for radial two-zone flow equations under the conditions of constant-head and partially penetrating well. J Hydraul Eng 2005;131(3):209–16.
[42] Yeh HD, Chen YJ, Yang SY. Semi-analytical solution for a slug test in partially penetrating wells including the effect of finite-thickness skin. Hydrol Process 2008;22:3741–8.
[43] Yeh HD, Yang SY, Peng HY. A new closed-form solution for a radial two-layer drawdown equation for groundwater under constant-flux pumping in a finite-radius well. Adv Water Resour 2003;26(7):747–57.
[44] Yeh HD, Yang SY. A novel analytical solution for a slug test conducted in a well with a finite-thickness skin. Adv Water Resour 2006;29(10):1479–89.